Nuclear sizes of ^{40,42,44,48}Ca from elastic scattering of 104 MeV alpha particles. I. Experimental results and optical potentials

H. J. Gils, E. Friedman,* H. Rebel, J. Buschmann, S. Zagromski, H. Klewe-Nebenius,[†] B. Neumann, R. Pesl, and G. Bechtold

Kernforschungszentrum Karlsruhe GmbH, Institut für Angewandte Kernphysik, P.O.B. 3640, D-7500 Karlsruhe, Federal Republic of Germany

Differential cross sections for elastic scattering of 104 MeV α particles from ^{40,42,44,48}Ca have been measured with high angular accuracy over a wide angular range. Optical model analysis based on a Fourier-Bessel description of the real potential reveals isotopic differences which, in particular for ^{48}Ca, indicate a small neutron skin.

> NUCLEAR REACTIONS $^{40,\ 42,\ 44,\ 48}$Ca(α,α), $E_\alpha = 104$ MeV, measured $\sigma(\theta)$; $\theta_{c.m.} = 3-110°$; enriched targets; optical model analysis using Fourier-Bessel method, deduced isotopic differences in the real potentials.

I. INTRODUCTION

One of the most important tests of current theories of nuclear structure is provided by investigations of the shape of the nucleon distributions. In general, however, the *matter* distribution of nuclei is less accessible experimentally than the nuclear *charge* distribution. The elastic scattering of strongly interacting particles has been suggested as a source of information on nuclear matter distributions. Due to the insufficient knowledge of the strong interaction, hadronic probes always imply the use of a model, either in an explicit or implicit form, when going from the phenomenologically observed interaction to the nucleon density distribution. Obviously the problem may be split into two parts: (i) How accurately can the phenomenological interaction potential between a probe particle and a target nucleus be determined? (ii) How reliable is the interpretation in terms of the nuclear density distributions? In addressing these questions the scattering of α particles in the 100 MeV energy region appears to be a most attractive method. In this energy region α particle scattering shows not only the well-known diffraction phenomena, which are characteristic for the absorption at the nuclear surface, but also a finite transparency of the nuclear interior due to the refractive property of the real potential.

As shown by Goldberg *et al.*[1] the α-particle–nucleus optical potential can be determined with a high degree of uniqueness if the range of the observed angular distribution extends beyond the "nuclear rainbow angle," which reflects sensitivity to the real potential at small radii. When the constraints due to the choice of a specific func-

tional form for the real optical potential are removed by introducing more flexible methods[2] (which correspond to the "model-independent" techniques in electron scattering analyses), one should be able to obtain reliable and accurate interaction potentials from sufficiently precise experimental data. The case of scattering from calcium isotopes is of particular interest. We find here not only an isotopic sequence ranging to a large neutron excess in ^{48}Ca and including two subsequent shell closures, but also a considerable amount of theoretical results and experimental information from other sources which may help to understand the connection between the optical potentials and the nuclear density distributions.

In this paper (I) we report the results of precision measurements of the elastic scattering of 104 MeV α particles from ^{40,42,44,48}Ca. The measured differential cross sections extend over a wide angular range and include the "nuclear rainbow" region as well as exceptionally small angles in order to increase the sensitivity also to the surface region. The analysis of the experimental data aims primarily at the determination of the strength and shape of the optical potentials, a good knowledge of which is a prerequisite for any further discussion of nuclear density distributions. In particular, the model dependence of the derived potentials which results from the use of simple functional forms is greatly reduced by applying the Fourier-Bessel (FB) method.[2] As compared to the conventional approaches the FB method is capable of revealing small isotopic differences in the interaction potentials and yields better descriptions of the differential cross sections. Additionally, it provides realistic estimates of the

uncertainties of the various extracted quantities.
A preliminary account of part of the present re-
sults (for [40,48]Ca) was already published.[3] A fur-
ther analysis of the present results in terms of
the nuclear density distributions of the calcium
isotopes invoking a density dependent folding mod-
el is the topic of the accompanying paper[4] (II).

II. EXPERIMENTAL

A. Setup and procedures

The experiments on [40,42,44,48]Ca were performed
at the scattering facility of the Karlsruhe Iso-
chronous Cyclotron[5] using 104 MeV α particles.
The targets were self-supporting metal foils of
natural Ca (96.9% [40]Ca) and highly enriched
[42,44,48]Ca (enrichment 94–99 %). The target thick-
nesses ranged between 1 and 5 mg/cm^2. The α-
particle beam was monochromized to about 50
keV full width at half maximum (FWHM) and fo-
cused to a beam spot of about 1.5 mm diameter at
the target position. From the emittance of the
cyclotron the angular divergence of the beam
(80% intensity) was estimated to be less than 0.20°.
The scattering chamber used has a diameter of
130 cm enabling us to obtain a small angular ac-
ceptance of ~ 0.15° with 1.5 mm slits in front of
the detectors; thus excessive slit scattering was
avoided. The scattered α particles were detected
by four Si surface barrier detectors of 4 mm
thickness mounted on a movable arm with angular
distances of 1.5° between each other. The elec-
tronic setup consisted of standard NIM modules
and a data acquisition system based on a NOVA II
computer.

The overall energy resolution of 150–180 keV
(FWHM) was sufficient to separate inelastic and
contaminant peaks (C,O) at almost all scattering
angles. Particle identification was not necessary
because the maximum energy loss of protons,
deuterons, and tritons in the detectors was less
than 43 MeV, far outside the energy region of
elastically scattered α particles. ^{3}He particles do
not interfere with the spectra because of the dis-
tinctly different Q values (about 15 MeV) com-
pared to α particles. Great efforts were focused
on the determination of the absolute zero point of
the scattering angle by measuring on both sides
of the beam (left-right measurement) and addi-
tionally by observing the kinematical behavior of
the carbon and oxygen target contamination peaks.

The total uncertainty of the scattering angles
was determined to be ±0.05°. At each scattering
angle the four targets were measured in turn in
order to avoid angular errors by new settings.
The elastic scattering cross sections were mea-
sured from $\theta_{c.m.} = 3°$ up to $\theta_{c.m.} = 110°$ in steps of

0.5° in the diffraction region ($\theta_{c.m.} \lesssim 60°$) and in
steps of 1.5° beyond. The beam current was mea-
sured by a Faraday cup behind the scattering
chamber and additionally monitored by a fixed
angle detector. The statistical errors were 1–2%
at most of the forward angles.

B. Results

Since the uncertainties of target thickness, inte-
grated beam current, and detector acceptance
determined the absolute scale of the cross sec-
tions only within 10% accuracy, the data were
finally normalized at forward angles to optical
model predictions (see Sec. III A). The normal-
ization factors were about 0.9 and agreed for all
isotopes within 2%. The uncertainty of the abso-
lute scattering angle was converted into cross
section errors by taking into account the slope of the
angular distributions. The experimental results
cover nine orders of magnitude as displayed in
Fig. 1. With increasing mass number one ob-
serves an increasing shift of the diffraction min-
ima towards smaller angles. The behavior of the
cross sections in the transition region between
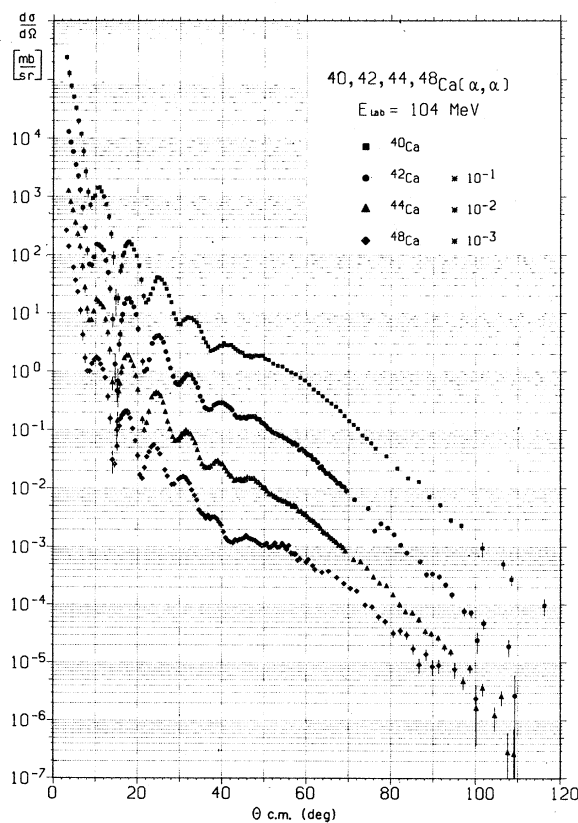
FIG. 1. Experimental differential cross sections for
the scattering of 104 MeV α particles from [40, 42, 44, 48]Ca.

diffraction and refraction and also the decrease at large angles are very similar for ^{40,42,44}Ca, whereas the transition structure and the slope of the refractive decrease in the case of ^{48}Ca slightly differ from those of the other isotopes. The measurements for ^{40}Ca and ^{48}Ca had been repeated over a period of one year with excellent reproducibility of the results to within 1%.

III. ANALYSIS

A. Conventional optical potentials

As a first step the analysis started with the conventional Woods-Saxon (WS) parametrization of the optical potential. Independent parameter sets were used for the real and imaginary parts, and the Coulomb potential was derived from realistic charge distributions of the projectile and target nuclei as determined from electron scattering experiments.[6] The best values of χ^2/F (χ^2 per degree of freedom) were significantly larger than 1, indicating that the WS optical potential was inadequate for describing the observed differential cross sections. This phenomenon had been noticed previously[7] with high-accuracy scattering data extending to large angles, and it was one of the motivations for the search for alternative forms of the optical potential.[7,2] It has become popular[7] recently to use the square of the WS function (WS^2) for the real potential. The difference between this form and the conventional WS form lies in the coupling between the surface region and the interior of the nucleus. We found indeed that the WS^2 form leads to better χ^2/F in fitting the measured data.

It is also obvious that the characteristic parameters depth, half-way radius, and skin thickness as well as the integral quantities obtained for each particular isotope are different for the alternatively used potential forms WS or WS^2, respectively. The differences between the integral quantities of the different isotopes, however, are rather independent from the choice of the functional form of the potential.

In a further step we introduced the WS^2 form also in the imaginary part of the optical potential. Thereby, the χ^2 values were only slightly reduced. Even if a surface absorption with three additional free parameters was included no further significant improvement of the theoretical description was achieved.[8] Therefore, we quote a real potential with WS^2 form and an imaginary potential with WS as the most reasonable description with conventional parametrization. These forms were also found to be most adequate in more fundamental treatments of the α-particle optical potential.[9,10] The final parameter values and some integral quantities of interest—the volume integral per nucleon pair $(-J/4A)$ and the root mean square (rms) radius—are compiled in Table I. These parameter values and, in particular, the corresponding differences between the various isotopes were rather insensitive against a shift of the absolute normalization of the cross sections (see Sec. II B) even by $\pm 10\%$.

B. Fourier-Bessel potentials

The WS^2 form is just another parametrization of the shape of the optical potential and, like the WS form, it cannot be considered suitable for studies of a series of isotopes since the choice of a particular simple functional form for the potential may introduce some bias into the results. In order to reduce such effects the real part of the optical potential U was written[2] more flexibly as

$$\mathrm{Re}U(r) = -V_0(r) - \sum_{n=1}^{N} b_n j_0\left(\frac{n\pi r}{R_c}\right), \qquad (1)$$

where $V_0(r)$ was either a WS or a WS^2 best fit potential and where the series of spherical Bessel functions was included only for $r \leq R_c$, with a suitably chosen cutoff radius R_c (usually 10–13 fm). The N coefficients b_n ($N \sim 10$–13) were obtained by adjustment to the experimental data. The imaginary potential was of the WS or WS^2 form and was adjusted simultaneously with the FB series. The term $V_0(r)$ served only as the initial potential for the FB fit. By using the FB analysis two main

TABLE I. Parameters of real WS^2 potential and imaginary WS potential.

A	Real potential					Imaginary potential					
	V_0 (MeV)	r_V (fm)	a_V (fm)	$-J_V/4A$ (MeV fm^3)	$\langle r_V^2 \rangle^{1/2}$ fm	W_0 (MeV)	r_W (fm)	a_W (fm)	$-J_W/4A$ (MeV fm^3)	$\langle r_W^2 \rangle^{1/2}$ fm	χ^2/F
40	152.6	1.404	1.253	317.9	4.315	20.3	1.603	0.678	100.9	4.938	3.7
42	138.1	1.446	1.196	312.1	4.372	22.3	1.603	0.653	109.2	4.952	4.1
44	139.4	1.438	1.189	310.0	4.394	24.0	1.578	0.665	112.6	4.973	3.6
48	162.1	1.378	1.274	318.6	4.458	18.9	1.633	0.603	95.0	5.114	3.3
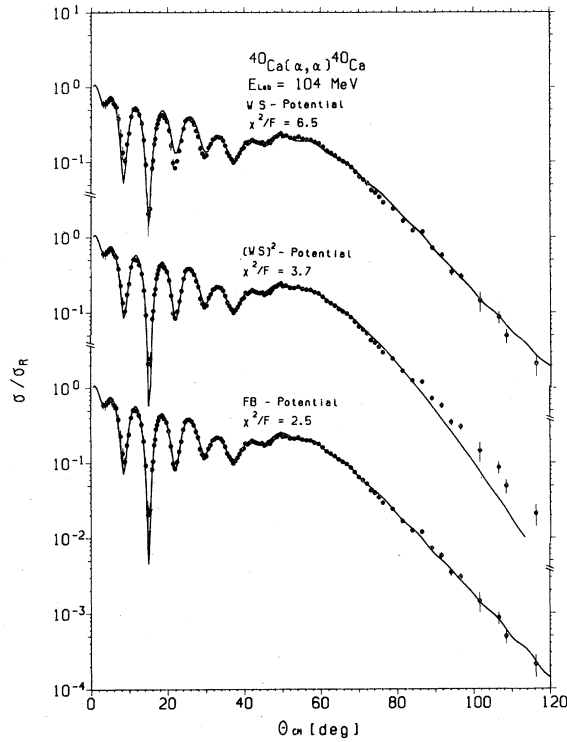
FIG. 2. Results of optical model analyses of 104 MeV
α-particle scattering from ^{40}Ca using different parame-
trizations.

FIG. 3. Results of the Fourier-Bessel method: Ex-
perimental and best-fit calculated differential cross sec-
tions.

goals are achieved[2]: (i) Sufficient flexibility is
introduced into the potential form thus allowing a
better description of the differential cross sec-
tions, whereby the constraints due to the choice of
particular functional forms of $V_0(r)$ are avoided.
(ii) Realistic estimates are obtained for the uncer-
tainties of various quantities such as the real pot-
ential itself, the volume integral, and the rms
radius. Uncertainties claimed for results of con-
ventional analyses are often underestimated[3] be-
cause the potential region to which the experimen-
tal data are not sensitive is simulated to be known
via the extrapolation of a particular functional
form.

Figure 2 displays examples of the fits obtained
for the ^{40}Ca data. The improvement in the fits

when going from WS to WS^2 and to the FB option is
clearly observed. Typical values of χ^2/F are
listed in the figure. It should be emphasized that
the shape of the imaginary potential was of the
WS or WS^2 form. That could have some residual
effect on the real potential although this effect is
found to be practically negligible.[8] Figure 3
shows FB fits to all four Ca isotopes and it dem-
onstrates the excellent description of the experi-
mental cross sections obtained with FB potentials.
Table II summarizes the results for integral quan-
tities of interest of the real (V) and imaginary (W)

TABLE II. Integral quantities of the FB potentials.

Target	χ^2/F	$-J_V/4A$ (MeVfm^3)	$\langle r_V^2 \rangle^{1/2}$ (fm)	$-J_W/4A$ (MeVfm^3)	$\langle r_W^2 \rangle^{1/2}$ (fm)
^{40}Ca	2.0	327 ± 2	4.37 ± 0.06	103	4.94
^{42}Ca	2.5	317 ± 3	4.38 ± 0.06	110	4.93
^{44}Ca	2.7	314 ± 3	4.41 ± 0.07	112	4.96
^{48}Ca	2.3	319 ± 5	4.49 ± 0.09	96	5.09

potentials. These were obtained from averaging various FB potentials with WS^2 form for the initial real potential V_0 and a WS form for the imaginary potential (see Table I).

IV. DISCUSSION

Although the FB method proved to be quite appropriate for the analysis of precisely measured elastic scattering cross sections extending to large scattering angles, the failure to reach χ^2/F values closer to 1 indicates some residual deficiency. As already mentioned, one possibility is, obviously, that the imaginary potential is not sufficiently flexible. But there are indications[8] that an additional flexibility of the imaginary potential (e.g. by introducing a surface term with three additional parameters) does not significantly improve the χ^2/F values. The results may also be affected by the coupling of the elastic scattering to inelastic channels. Explicitly including such effects by a coupled channel analysis could possibly further reduce the values of χ^2/F. It should be remembered, however, that the description of the scattering cross sections on the basis of a local potential is, in itself, an approximation. It is not unlikely that values of $\chi^2/F \sim 1$ cannot be achieved at all for high precision data within such an approach.

The results of the present work provide information on differences between the α-particle–nucleus optical potentials for the calcium isotopes. In Fig. 4 the differences between the real parts normalized to their respective volume integral are shown in analogy with similar curves usually presented for the charge distributions.

The approximate equality of the volume integral per nucleon pair of the real potential ($J_V/4A$ in Table II) suggests a folding model[11] interpretation. A folding model with a density independent effective interaction leads to a constant value of $J_V/4A$. This condition is not met exactly by the results of the FB fits. The small deviations may indicate some density dependence of the microscopic interaction, which also implies that the additivity of the mean square radii of the α-particle–nucleon effective interaction $\langle r_{\alpha N}^2 \rangle$ and of the nuclear density distribution $\langle r_m^2 \rangle$

$$\langle r_{\alpha N}^2 \rangle + \langle r_m^2 \rangle = \langle r_{\text{pot}}^2 \rangle \qquad (2)$$

(which holds in a density independent folding model) has to be considered only as an approximation.

The study of nuclear density distributions and nuclear sizes is the topic of the following paper[4] where the above questions will be discussed in detail. In particular it will be shown that the additivity of the mean square radii remains quite reli-
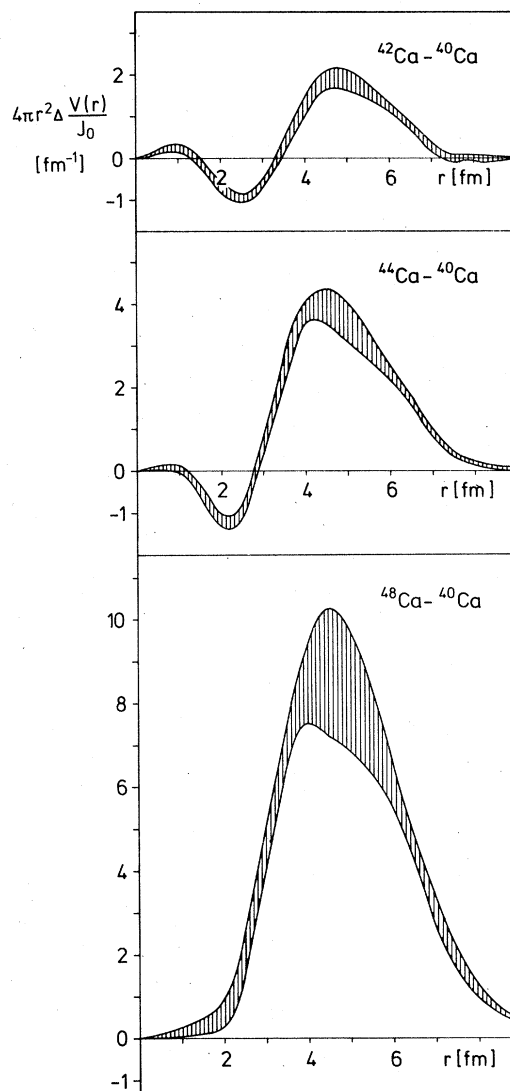
FIG. 4. Differences between real potentials obtained from the Fourier-Bessel analysis of 104 MeV α-particle scattering.

able. Anticipating the justification[4,12] of Eq. (2), and introducing the information about the charge distribution[13] the difference of the rms radii of the real potentials reflects a small neutron skin of ^{48}Ca.

*The Racah Institute of Physics, The Hebrew University, Jerusalem, Israel.

†Kernforschungszentrum Karlsruhe GmbH, Institut für Radiochemie.

[1] D. A. Goldberg and S. M. Smith, Phys. Rev. Lett. 29, 500 (1972).

[2] E. Friedman and C. J. Batty, Phys. Rev. C 17, 34 (1978).

[3] E. Friedman, H. J. Gils, H. Rebel, and Z. Majka, Phys. Rev. Lett. 41, 1220 (1978).

[4] H. J. Gils, E. Friedman, Z. Majka, and H. Rebel, following paper, Phys. Rev. C 21, 1245 (1980).

[5] H. Rebel, G. W. Schweimer, G. Schatz, J. Specht, R. Löhken, G. Hauser, D. Habs, and H. Klewe-Nebenius, Nucl. Phys. A182, 145 (1972).

[6] C. W. de Jager, H. de Vries, and C. de Vries, At. Data Nucl. Data Tables 14, 479 (1974).

[7] A. Budzanowski, K. Grotowski, M. Grzywacz, and A. Strzalkowski, Progress Report, Institute for Nuclear Physics, Cracow, 1972 (unpublished); D. A. Goldberg, Phys. Lett. 55B, 59 (1975).

[8] H. J. Gils, E. Friedman, H. Rebel, J. Buschmann, S. Zagromski, H. Klewe-Nebenius, B. Neumann, R. Pesl, and G. Bechtold, Report No. KfK 2838, Kernforschungszentrum Karlsruhe, 1979 (unpublished).

[9] Z. Majka, H. J. Gils, and H. Rebel, Z. Physik A288, 139 (1978).

[10] N. Vinh Mau, Phys. Lett. 71B, 5 (1977).

[11] A. M. Bernstein, *Advances in Nuclear Physics*, edited by M. Baranger and E. Vogt (Plenum, New York, 1969); D. F. Jackson and V. K. Kembhavi, Phys. Rev. 178, 1626 (1969).

[12] Z. Majka, H. J. Gils, and H. Rebel, Acta Phys. Pol. (to be published), and in *What do we know about the radial shape of nuclei in the Ca-region?*, edited by H. Rebel, H. J. Gils, and G. Schatz (Kernforschungszentrum Karlsruhe, Karlsruhe, 1979).

[13] H. D. Wohlfahrt and J. Friedrich, private communication, and in *What do we know about the radial shape of nuclei in the Ca-region?*, edited by H. Rebel, H. J. Gils, and G. Schatz (Kernforschungszentrum Karlsruhe, Karlsruhe, 1979).